· Original article ·

Predictive index based on minimum corneal thickness and symmetry index back of Sirius for early diagnosis of keratoconus

Yue Xu[1,2], *Ya-Ru Ren*[1], *Xin-Yu Zhuang*[1], *Xiao-Feng Zhang*[1,2]

引用:徐悦,任亚茹,庄歆予,等. 基于 Sirius 角膜最薄点厚度和后表面曲率对称指数的预测指标诊断早期圆锥角膜. 国际眼科杂志 2022;22(9):1426-1435

[1]Department of Ophthalmology, the First Affiliated Hospital of Soochow University, Suzhou 215000, Jiangsu Province, China; [2]Department of Ophthalmology, Dushu Lake Hospital Affiliated to Soochow University, Suzhou 215000, Jiangsu Province, China

Correspondence to: Xiao-Feng Zhang. Department of Ophthalmology, the First Affiliated Hospital of Soochow University, Suzhou 215000, Jiangsu Province, China; Department of Ophthalmology, Dushu Lake Hospital Affiliated to Soochow University, Suzhou 215000, Jiangsu Province, China. zhangxiaofeng@suda.edu.cn

Received: 2021-04-01 Accepted: 2022-07-21

基于 Sirius 角膜最薄点厚度和后表面曲率对称指数的预测指标诊断早期圆锥角膜

徐 悦[1,2],任亚茹[1],庄歆予[1],张晓峰[1,2]

作者单位:[1](215000)中国江苏省苏州市,苏州大学附属第一医院眼科;[2](215000)中国江苏省苏州市,苏州大学附属独墅湖医院眼科

作者简介:徐悦,毕业于苏州大学,硕士,住院医师,研究方向:角膜眼表疾病。

通讯作者:张晓峰,毕业于苏州大学,博士,主任医师,副教授,研究方向:角膜眼表疾病. zhangxiaofeng@suda.edu.cn

摘要

目的:构建和验证基于 Sirius 眼前节分析仪参数的圆锥角膜早期诊断模型。

方法:该研究包括预测队列中的 46 只早期圆锥角膜眼(34 例患者的 20 只右眼和 26 只左眼)和 46 只年龄和性别相匹配的正常眼(46 例患者均为右眼)。基于 Sirius 的地形图、厚度和像差变量,使用 LASSO 和 Logistic 回归分析构建预测指数。应用队列包括 23 只被 Sirius 归类为可疑圆锥角膜病例的早期圆锥角膜眼(23 例患者的 12 只右眼和 11 只左眼)和 23 只年龄和性别相匹配的正常眼(23 例患者均为右眼)。在应用队列中对预测指标进行了外部验证。

结果:Sirius 圆锥角膜指数(SKI)是由 Sirius 角膜最薄点厚度和后表面曲率对称指数计算得出。Logistic 回归分析后,SKI 在预测队列中具有最高的 AUC 值(AUC=0.932)。SKI 的截止值设定为 0.44。随后,详细分析了预测队列的受试者工作特征(ROC)曲线、校准图和诊断公式的列线图。最后,在应用队列中评估了 SKI 的准确性,其敏感性为 91%,特异性为 96%。

结论:基于 Sirius 角膜最薄点厚度和后表面曲率对称指数的 SKI 是屈光手术术前筛查中早期发现圆锥角膜的一种简单而有效的方法。

关键词:Sirius 圆锥角膜指数;早期圆锥角膜;角膜最薄点厚度;后表面曲率对称指数;Sirius

Abstract

• AIM: To construct and validate a diagnostic model for early detection of keratoconus based on parameters in Sirius.

• METHODS: The study comprised of 46 early keratoconus eyes (including 20 right eyes and 26 left eyes in 34 patients) and 46 age- and gender-matched normal eyes (including the right eyes of 46 patients) in the prediction group. The predictive index was constructed using LASSO and Logistic regression analyses based on the topographic, pachymetric and aberrometry variables of Sirius. There were 23 early keratoconus eyes categorized as suspected keratoconus cases by Sirius (including 12 right eyes and 11 left eyes in 23 patients) and 23 age- and gender-matched normal eyes (including the right eyes of 23 patients) included in the application cohort. External validation of predictors was performed for the application cohort.

• RESULTS: Sirius Keratoconus Index (SKI) was calculated based on the minimum corneal thickness and symmetry index back of Sirius. Highest AUC values were obtained in the prediction group (AUC = 0.932) after Logistic regression analysis. The cut-off value of SKI was set at 0.44. Then, the receiver operating characteristic (ROC) curve, calibration plot and nomogram of the diagnostic formula were analyzed for the prediction cohort in detail. Finally, the accuracy of the SKI was evaluated in the application cohort; the sensitivity was 91% and the specificity was 96%.

• CONCLUSION: SKI based on minimum corneal thickness and symmetry index back of Sirius is a simple and effective method for early detection of keratoconus in the preoperative screening for refractive surgery.

• KEYWORDS: Sirius keratoconus index; early keratoconus; minimum corneal thickness; symmetry index back; Sirius

DOI:10.3980/j.issn.1672-5123.2022.9.03

Citation: Xu Y, Ren YR, Zhuang XY, *et al*. Predictive index based on minimum corneal thickness and symmetry index back of Sirius for early diagnosis of keratoconus. *Guoji Yanke Zazhi* (*Int Eye Sci*) 2022;22(9):1426-1435

INTRODUCTION

Keratoconus (KC) is a progressive, bilateral and asymmetrical corneal ectatic disorder that may lead to severe visual impairment[1-3]. Early diagnosis of KC is important in corneal refractive surgery[4]. In general, early KC eyes lack the characteristic slit-lamp microscopy signs [5]. Previous studies suggest that abnormal posterior corneal surface and alteration in corneal thickness progression are necessary for early diagnosis of KC[6]. On the contrary, Reddy *et al*.[7] show that anterior curvature parameters, are better for distinguishing early KC from normal eyes. It is therefore, important to determine the efficacy of various parameters and construct an effective index for evaluation of early KC diagnosis.

Sirius (CSOInc, Florence, Italy), a combination of the Scheimpflug and Placido topography systems, provides a comprehensive evaluation of the anterior, posterior corneal surface and corneal thickness[8-9]. Although multiple parameters for evaluating the cornea and early diagnosing of KC have been proposed, a proper index for distinguishing early KC from the normal eyes remains unknown[10-12]. This study aimed at constructing an efficient formula and index for early diagnosis of KC. External validation was also performed; accuracy of the formula and index were further evaluated.

MATERIALS AND METHODS

Ethics Approval Protocols in this retrospective study were approved by the ethics committee of the First Affiliated Hospital of Soochow University and they adhered to the tenets of the Declaration of Helsinki. Patient information was anonymized.

Study Cohorts KC group was diagnosed based on the combination of clinical and topographic examinations, including slit lamp, corneal topography and Sirius. Two criteria for evaluation of early KC diagnosis were set: The eyes can be diagnosed as early KC eyes according to corresponding corneal topographic features including local corneal steepening and asymmetric astigmatism, or the contralateral eye was diagnosed as KC and included as an early KC eye even in absence of any obvious KC-related corneal topographic changes and when the vision could still be corrected using frame glasses; Early KC eye was defined as per Amsler-Krumeich classification (stage 1: average K value <48D and corneal cylinder <5D)[5].

The normal group consisted of refractive surgery candidates with normal clinical and topographic features[11]. The right eye of each of the normal subjects was included in analyses for normal group.

The inclusion criteria for KC patients in the prediction cohort were as follows: 1) patients under the age of 60 who had visited the ophthalmology department of the First Affiliated Hospital of Soochow University between August 2016 and July 2020; 2) KC patients diagnosed for stage 1 KC according to Amsler-Krumeich classification; 3) absence of any other ocular diseases except keratoconus and refractive error; 4) no history of ocular surgeries. A total of 34 early KC patients (46 eyes) and 46 age- and gender-matched normal subjects (46 eyes) were thus enrolled in the prediction cohort.

The application cohort was an independent group for external validation of the diagnostic index, consisting of early KC eyes categorized as suspected KC cases by Sirius, and age-and gender-matched normal eyes. KC patients in the application cohort also conformed to the inclusion criteria as in the prediction cohort. A total of 23 early KC patients (23 eyes) and 23 age- and gender-matched normal subjects (23 eyes) were enrolled in the application cohort.

Data Extraction There were 6 topographic parameters including steep K, flat K, the average K, cylinder, corneal surface regularity index (SRI) and corneal surface asymmetry index (SAI) extracted from the corneal topography measured by TMS-4 (Tomey, Japan). Using Sirius, the 20 parameters which were measured are as follows: 1) Pachymetric parameters: central corneal thickness (CCT), minimum corneal thickness (MCT), the difference between CCT and MCT (δCT), corneal volume, symmetry index front (SIf), which was the difference between the average anterior tangential curvature of the two circular zones (of radius 1.5mm) centered on the vertical axis in the inferior and superior hemispheres, and symmetry index back (SIb), which was the difference between the average posterior tangential curvature of the two circular zones (of radius 1.5mm) centered on the vertical axis in the inferior and superior hemispheres; 2) Aberrometry parameters: anterior zone of 6mm root mean square values per unit area (A6 RMS/A), posterior zone of 6mm root mean square values per unit area (P6 RMS/A), anterior zone of 8mm root mean square values per unit area (A8 RMS/A), posterior zone of 8mm root mean square values per unit area (P8 RMS/A), high order aberration (HOA), Baiocchi-Calossi-Versaci index (BCV), Baiocchi-Calossi-Versaci index front (BCVf), Baiocchi-Calossi-Versaci index back (BCVb), coma, vertical trefoil [Z(3,-3)], vertical coma [Z(3,-1)], horizontal coma [Z(3,1)], oblique trefoil [Z(3,3)] and spherical aberration [Z(4,0)].

ROC Curve Analysis Receiver operating characteristic (ROC) curve was used to determine the accuracy and predictive value of each parameter by comparing the area under the curve (AUC) for the KC group with the normal group in the prediction cohort. The optimal cut-off value for each parameter was estimated based on a uniform computing index (Youden index). The diagnosis probability as calculated using the formula of the prediction group was termed as "Sirius Keratoconus Index" (SKI). ROC curve analysis of SKI, and that of each of the parameters of SKI was performed and their AUCs were compared between the prediction and the application cohort. Sensitivity, specificity,

positive and negative likelihood ratios, positive and negative predictive values were determined for the different parameters of the prediction cohort.

Statistical Analysis The statistical analysis was performed using SPSS software (version 25.0; IBM Corp., New York, NY, USA). Normality of the data distribution was examined using the Kolmogorov-Smirnov test and compared using Student's *t*-test (normal distribution) or Mann-Whitney U test (for data not conforming to normal distribution). Pearson correlation coefficients (r) were used to determine the correlation between different parameters. Least Absolute Shrinkage and Selection Operator (LASSO) regression analysis was used for parameter selection for further analysis and regularization[13-14]. LASSO regression analysis was performed using glmnet package in R (Version 3.6.0) and RStudio (Version 1.2.1335)[15]. The Logistic regression analysis was performed for all the parameters that were selected as independent variables from LASSO analysis. The formula was then constructed and evaluated by calibration plot based on Hosmer-Lemeshow goodness-of-fit test. A calibration plot along the 45-degree line was suggestive of high consistency between the expected and observed results in the model. The rms package in R was used to visualize the nomogram of the model based on the independent variables selected from the prediction group. For all analyses, two-sided *P*-values less than 0.05 were considered statistically significant.

RESULTS

This study was conducted in three stages; Depicts the flowchart of the construction and application of the formula for early diagnosis of keratoconus. First, the formula and SKI were determined using 25 keratoconus-related parameters; with LASSO regression and Logistic regression analyses, these parameters were calculated for the prediction group. ROC curve, calibration plot and nomogram of the formula were evaluated in the prediction group. External validation by ROC curve and calibration plot were analyzed for the application cohort (Figure 1).

Overall Comparison between Keratoconus and Normal Groups in the Prediction Cohort The demographic, topographic, pachymetric and aberrometry parameters of the prediction cohort (34 early KC patients (46 eyes) and 46 comparable normal subjects (46 eyes)) are presented in Table 1. The age ($P=0.961$) and gender ($P=0.725$) were comparable between the KC group and normal group. A total of 25 keratoconus-related parameters, except Z (3, 3), showed significant differences between the KC group and normal group by Student's *t*-test or Mann-Whitney U test ($P<0.05$). Correlation analysis of 28 keratoconus-related parameters was displayed for the KC group and normal group in the prediction cohort (Figure 2A-B). There were 16 parameters including 2 topographic (SRI and SAI), 3 pachymetric and 11 aberrometry parameters showed a significant positive correlation with other parameters (cor.>0.4, $P<0.001$) in the keratoconus group. In addition, Z (3, -1) showed a significant negative correlation with other parameters (cor.<-0.4, $P<0.001$) in keratoconus group. Few parameters showed significant correlation in normal group.

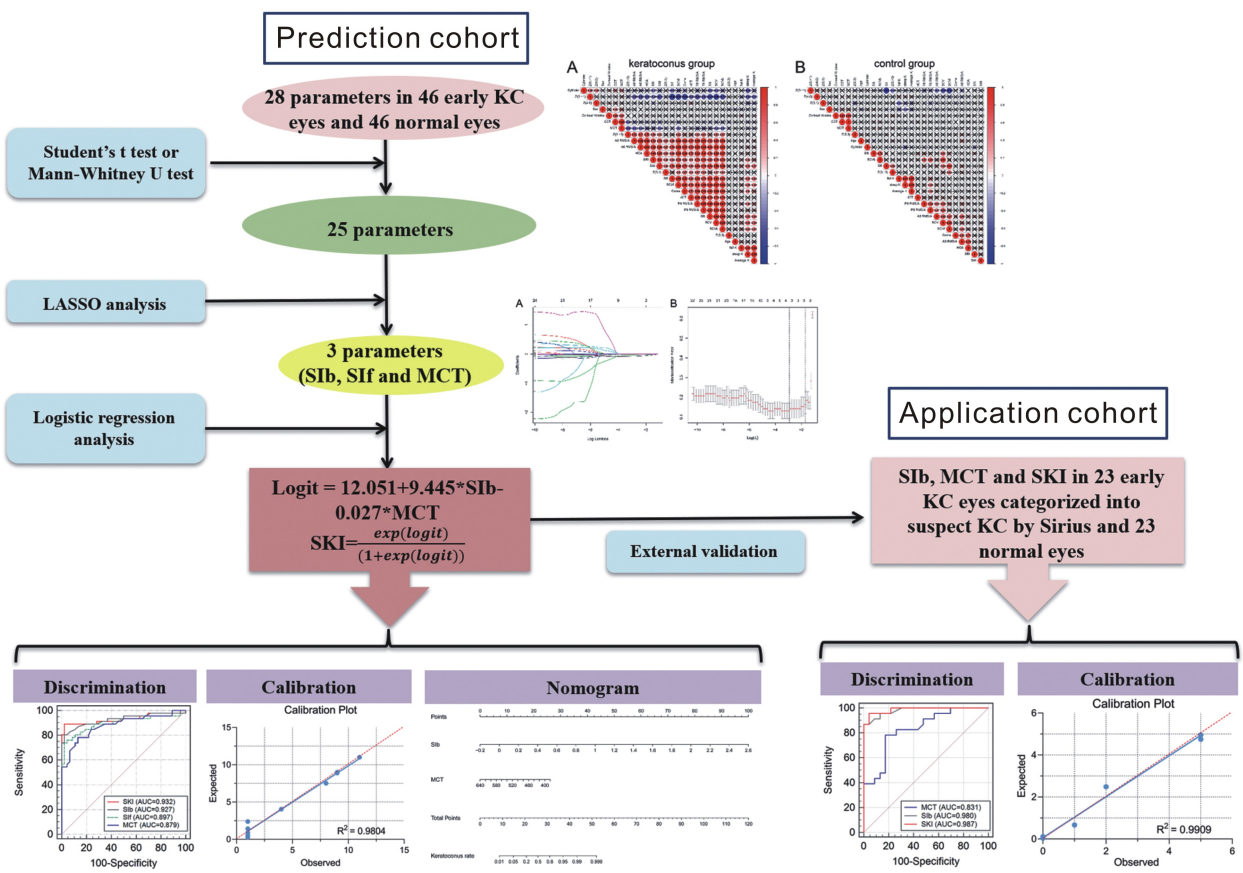

Figure 1 Flowchart showing the construction and application of the formula for early diagnosis of keratoconus in this study.

Table 1 Comparative demographic, topographic, pachymetric and aberrometry parameters in the prediction cohort

Parameters	Keratoconus group	Normal group	*P*
Number (eyes)	46	46	
Age (years)	22.00 (17.75, 28.50)	21.50 (20.00, 25.00)	0.961
Gender (male:female)	27:7	35:11	0.725
steep K ($\bar{x}\pm s$, D)	45.42±2.17	43.87±1.66	<0.001
flat K ($\bar{x}\pm s$, D)	43.24±1.69	42.48±1.48	0.025
Average K ($\bar{x}\pm s$, D)	44.33±1.84	43.18±1.53	0.002
Cylinder (D)	−1.84 (−2.67, −1.10)	−1.41 (−1.79, −0.86)	0.002
SRI	0.24 (0.09, 0.59)	0.07 (0.05, 0.16)	<0.001
SAI	0.74 (0.38, 1.97)	0.26 (0.19, 0.41)	<0.001
CCT ($\bar{x}\pm s$, μm)	496.83±40.37	549.30±30.62	<0.001
MCT (μm)	483.50 (463.75, 512.25)	549.00 (530.50, 564.25)	<0.001
δCT (μm)	6 (4, 15.5)	2 (1, 4.25)	<0.001
Corneal Volume ($\bar{x}\pm s$, mm^3)	55.87±3.51	59.03±3.30	<0.001
SIf ($\bar{x}\pm s$, D)	2.52±2.19	−0.06±0.49	<0.001
SIb (D)	0.71 (0.26, 1.43)	0.03 (−0.01, 0.13)	<0.001
A6 RMS/A (μm/mm^2)	0.10 (0.04, 0.16)	0.02 (0.02, 0.03)	<0.001
P6 RMS/A (μm/mm^2)	0.24 (0.14, 0.46)	0.09 (0.08, 0.11)	<0.001
A8 RMS/A (μm/mm^2)	0.10 (0.05, 0.15)	0.04 (0.03, 0.05)	<0.001
P8 RMS/A (μm/mm^2)	0.23 (0.17, 0.36)	0.14 (0.11, 0.19)	<0.001
HOA (μm)	0.84 (0.53, 1.41)	0.38 (0.33, 0.45)	<0.001
BCV (D)	1.11 (0.33, 2.24)	0.10 (0.00, 0.22)	<0.001
BCVf (D)	1.11 (0.40, 2.16)	0.09 (0.00, 0.21)	<0.001
BCVb (D)	1.01 (0.45, 2.34)	0.10 (0.00, 0.29)	<0.001
Coma (μm)	0.58 (0.33, 1.18)	0.17 (0.12, 0.27)	<0.001
Z (3, −3) (μm)	0.18 (−0.07,0.37)	−0.06 (−0.17, 0.06)	0.001
Z (3, −1) (μm)	−0.43 (−1.00, −0.12)	0.08 (−0.03, 0.22)	<0.001
Z (3, 1) (μm)	0.09 (−0.14, 0.27)	−0.04 (−0.10, 0.01)	0.012
Z (3, 3) (μm)	−0.03 (−0.25, 0.14)	−0.03 (−0.11, 0.03)	0.870
Z (4, 0) (μm)	0.14 (0.06, 0.22)	0.20 (0.17, 0.25)	0.004

D: Diopters; SRI: Surface regularity index; SAI: Surface asymmetry index; CCT: Central corneal thickness; MCT: Minimum corneal thickness; δCT: the difference between CCT and MCT; SIf: Symmetry index front; SIb: Symmetry index back; A6 RMS/A: Anterior 6mm zone root mean square values per unit area; P6 RMS/A: Posterior 6mm zone root mean square values per unit area; A8 RMS/A: Anterior 8mm zone root mean square values per unit area; P8 RMS/A: Posterior 8mm zone root mean square values per unit area; HOA: High order aberration; BCV: Baiocchi-Calossi-Versaci index; BCVf: Baiocchi-Calossi-Versaci index front; BCVb: Baiocchi-Calossi-Versaci index back; Z (3, −3): Vertical trefoil; Z (3, −1): Vertical coma; Z (3, 1): Horizontal coma; Z (3, 3): Oblique trefoil; Z (4, 0): Spherical aberration.

LASSO Regression Analysis in the Prediction Cohort

LASSO regression analysis was performed for 25 significant parameters in prediction cohort. LASSO coefficient profile is shown in Figure 2C. The calculation of the tuning parameter (λ) in the LASSO model is shown in Figure 2D. The y-axis represents partial likelihood deviance; The lower x-axis, log (λ) and the upper x-axis, the average number of predictors. The red dots represent the average deviance values for each model with a given λ, where the model is the best fit to data. Thus, vital keratoconus-related parameters including SIb, SIf, and MCT were selected.

LASSO, Least Absolute Shrinkage and Selection Operator; SRI, surface regularity index; SAI, surface asymmetry index; δCT, the difference between CCT and MCT; SIf, symmetry index front; SIb, symmetry index back; A6 RMS/A, anterior 6mm zone root mean square values per unit area; P6 RMS/A, posterior 6mm zone root mean square values per unit area; A8 RMS/A, anterior 8mm zone root mean square values per unit area; P8 RMS/A, posterior 8mm zone root mean square values per unit area; HOA, high order aberration; BCV, Baiocchi-Calossi-Versaci index; BCVf, Baiocchi-Calossi-Versaci index front; BCVb, Baiocchi-Calossi-Versaci index back; Z (3, −3), vertical trefoil; Z (3, 1), horizontal coma; Z (3, −1), vertical coma; MCT, minimum corneal thickness.

Correlation analysis of 28 keratoconus-related parameters was displayed in keratoconus group and normal group of prediction cohort. 16 parameters, including 2 topographic (SRI and SAI), 3 pachymetric (δCT, SIf, and SIb) and 11 aberrometry parameters (A6 RMS/A, P6 RMS/A, A8 RMS/A, P8 RMS/A, HOA, BCV, BCVf, BCVb, Coma, Z (3, −3) and Z (3, 1)), showed positive correlation with other

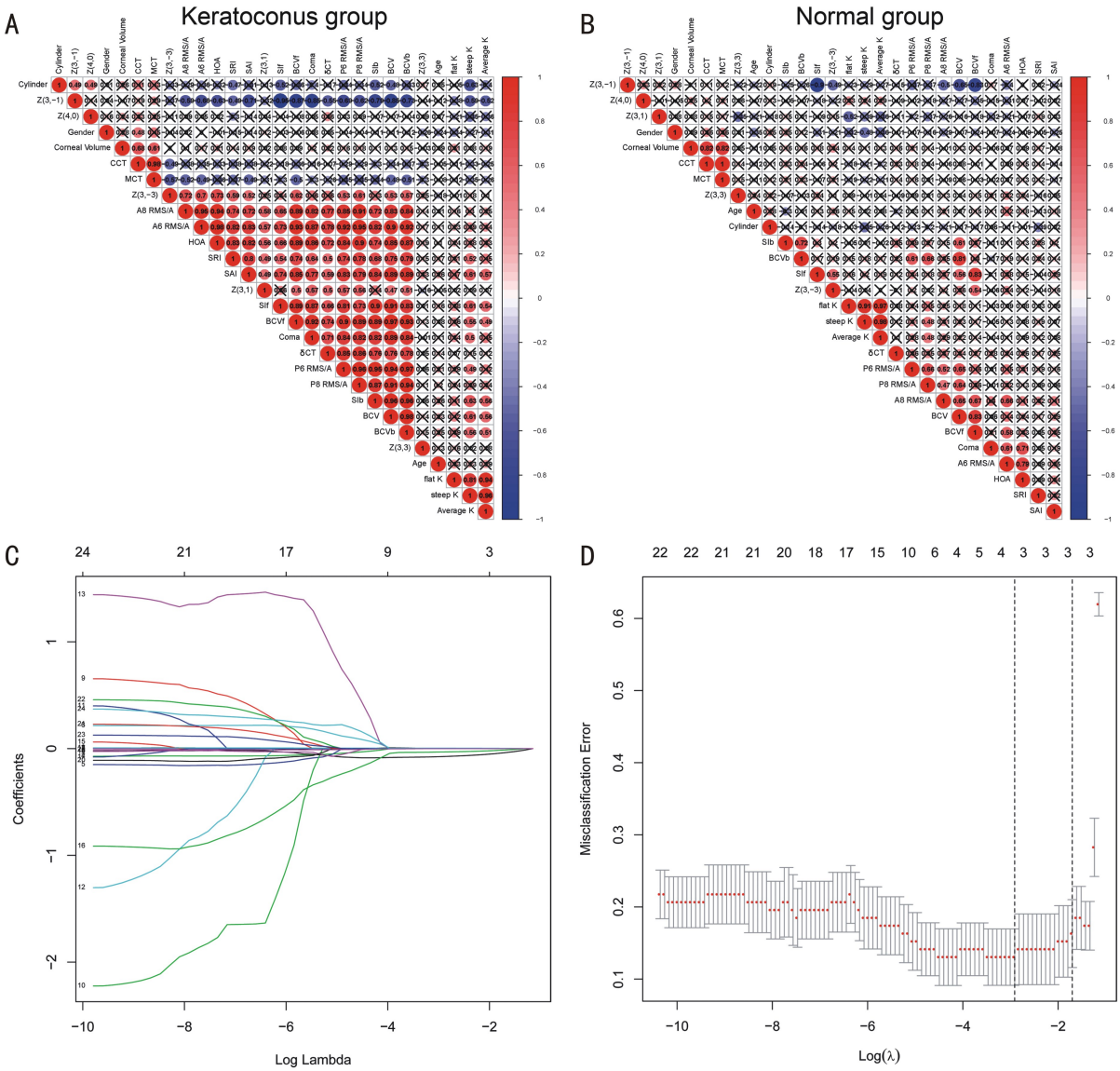

Figure 2 Correlation and LASSO regression analysis of keratoconus-related parameters in prediction cohort.

parameters (cor.>0.4, $P<0.001$) in keratoconus group. In addition, Z (3, -1) showed negative correlation with other parameters (cor.<-0.4, $P<0.001$) in keratoconus group. Few parameters showed significant correlation with others in normal group (Figure 2A - B). LASSO regression analysis was performed in 25 significant parameters selected by Student's *t* test or Mann - Whitney U test in prediction group. LASSO coefficient profile was visualized (Figure 2C). The selection of the tuning parameter (λ) in the LASSO model was calculated, and 3 parameters (SIb, SIf, and MCT) were selected out for further analysis (Figure 2D).

Multivariate Logistic Regression Analysis in the Prediction Cohort The multivariate Logistic regression analysis was performed for the prediction group on the basis of SIb, SIf, and MCT (Table 2). SIb and MCT were selected as explanatory parameters to predict early KC in patients. The regression coefficients of SIb and MCT were 9.445 and -0.027, respectively. The prediction formula was calculated as follows: logit = 12.051+9.445×SIb (D) -0.027×MCT(μm).

Table 2 Results of multivariate Logistic regression analysis

Parameters	Regression coefficient	SE	Wald	*P*
Constant	12.051	5.684	4.495	0.0340
SIb	9.445	3.040	9.652	0.0019
MCT	-0.027	0.011	6.197	0.0128

SE: Standard error; Wald: Wald statistic; SIb: Symmetry index back; MCT: Minimum corneal thickness.

The probability of early diagnosis based on Sirius parameters was termed "SKI" and calculated by the following conversion formula: $SKI = \frac{exp(logit)}{(1 + exp(logit))}$.

ROC Curve, Calibration Analysis and Nomogram in the Prediction cohort Present ROC analysis, sensitivity, specificity, positive and negative likelihood ratios, positive and negative predictive values for 25 keratoconus - related parameters and SKI to differentiate the early KC from normal eyes in the prediction cohort were shown in Table 3 and supplementary Table 1. The ROC curve represents the relationship

Table 3 ROC analysis, sensitivity and specificity for different parameters to differentiate early keratoconus from normal eyes in the prediction cohort

Parameters	AUC	SE	95%*CI*	*P*	Youden index (J)	Cut-off	Sensitivity (%)	Specificity (%)
steep K (D)	0.710	0.05	0.605-0.799	0.0001	0.370	>44.83	60.87	76.09
flat K (D)	0.630	0.06	0.527-0.732	0.0226	0.280	>44.45	34.78	93.48
Average K (D)	0.681	0.06	0.576-0.774	0.0012	0.304	>43.77	63.04	67.39
Cylinder (D)	0.685	0.06	0.580-0.778	0.0009	0.370	≤-1.68	65.22	71.74
SRI	0.764	0.05	0.664-0.846	<0.0001	0.413	>0.10	73.91	67.39
SAI	0.868	0.04	0.781-0.929	<0.0001	0.630	>0.51	65.22	97.83
CCT (μm)	0.852	0.04	0.763-0.918	<0.0001	0.587	≤516.00	71.74	86.96
MCT (μm)	0.879	0.04	0.794-0.938	<0.0001	0.652	≤513.00	78.26	86.96
δCT (μm)	0.804	0.05	0.709-0.880	<0.0001	0.500	>3.00	82.61	67.39
Corneal Volume (mm^3)	0.740	0.05	0.638-0.826	<0.0001	0.435	≤56.00	63.04	80.43
SIf (D)	0.897	0.04	0.815-0.950	<0.0001	0.717	>0.59	76.09	95.65
SIb (D)	0.927	0.03	0.853-0.971	<0.0001	0.783	>0.21	80.43	97.83
A6 RMS/A ($\mu m/mm^2$)	0.907	0.03	0.829-0.958	<0.0001	0.761	>0.03	86.96	89.13
P6 RMS/A ($\mu m/mm^2$)	0.900	0.03	0.820-0.953	<0.0001	0.717	>0.13	76.09	95.65
A8 RMS/A ($\mu m/mm^2$)	0.866	0.04	0.779-0.928	<0.0001	0.587	>0.05	73.91	84.78
P8 RMS/A ($\mu m/mm^2$)	0.789	0.05	0.691-0.867	<0.0001	0.435	>0.19	60.87	82.61
HOA (μm)	0.869	0.04	0.782-0.930	<0.0001	0.652	>0.54	73.91	91.30
BCV (μm)	0.898	0.03	0.818-0.952	<0.0001	0.696	>0.25	84.78	84.78
BCVf (D)	0.896	0.04	0.814-0.950	<0.0001	0.717	>0.31	84.78	86.96
BCVb (D)	0.889	0.03	0.806-0.945	<0.0001	0.674	>0.55	69.57	97.83
Coma (μm)	0.855	0.04	0.767-0.920	<0.0001	0.674	>0.30	80.43	86.96
Z (3, -3) (μm)	0.699	0.06	0.594-0.790	0.0004	0.413	>0.15	52.17	89.13
Z (3, -1) (μm)	0.884	0.04	0.801-0.942	<0.0001	0.696	≤-0.20	73.91	95.65
Z (3, 1) (μm)	0.651	0.06	0.545-0.748	0.0156	0.413	>0.06	52.17	89.13
Z (4, 0) (μm)	0.676	0.06	0.571-0.770	0.0032	0.391	≤0.13	50.00	89.13
SKI	0.932	0.03	0.860-0.974	<0.0001	0.870	>0.44	89.13	97.83

ROC: Receiver operating characteristic; AUC: Area under the curve; SE: Standard error; 95%*CI*: 95% confidence interval; D: Diopters; SRI: Surface regularity index; SAI: Surface asymmetry index; CCT: Central corneal thickness; MCT: Minimum corneal thickness; δCT: the difference between CCT and MCT; SIf: Symmetry index front; SIb: Symmetry index back; A6 RMS/A: Anterior 6mm zone root mean square values per unit area; P6 RMS/A: Posterior 6mm zone root mean square values per unit area; A8 RMS/A: Anterior 8mm zone root mean square values per unit area; P8 RMS/A: Posterior 8mm zone root mean square values per unit area; HOA: High order aberration; BCV: Baiocchi-Calossi-Versaci index; BCVf: Baiocchi-Calossi-Versaci index front; BCVb: Baiocchi-Calossi-Versaci index back; Z (3, -3): Vertical trefoil; Z (3, -1): Vertical coma; Z (3, 1): Horizontal coma; Z (3, 3): Oblique trefoil; Z (4, 0): Spherical aberration; SKI: Sirius Keratoconus Index.

between sensitivity of the discriminant test and its false-positive rate (1-specificity). AUC and Youden's index (J) were computed to evaluate the bias in these parameters. Markedly, the AUC of SKI (sensitivity = 89% and specificity = 98%, AUC = 0.932) was the highest in the prediction cohort. The ROC curve plot delineated the sensitivity and specificity of the 3 parameters (SIb, SIf and MCT) after LASSO regression analysis and SKI (Figure 3A). SKI (AUC = 0.932) was calculated on the basis of SIb (AUC = 0.927) and MCT (AUC = 0.879) after Logistic regression analysis. The cut-off value for SKI was determined at 0.44.

Calibration plot of SKI was constructed for the prediction cohort using Hosmer-Lemeshow goodness-of-fit test, with the red dotted line as the reference line. The curve of the prediction cohort deviated slightly from the reference line; A good calibration of SKI was estimated in 92% of cases (R^2 = 0.9804) (Figure 3B).

In addition, a nomogram was constructed based on SIb and MCT to predict the probability of early keratoconus (Figure 3C). A vertical line was drawn upward from each parameter and the corresponding points were recorded. The points at each of the parameters were summed up to calculate the total score which corresponded to the predicted probability of keratoconus at the bottom of the nomogram.

The ROC curve analysis delineated the sensitivity and specificity of 3 parameters (SIb, SIf, and MCT) after LASSO regression analysis and SKI. SKI was calculated on the basis of SIb and MCT byLogistic regression analysis and had the highest AUC among all the 25 parameters (Figure 3A). Calibration plot was constructed in prediction group, with the

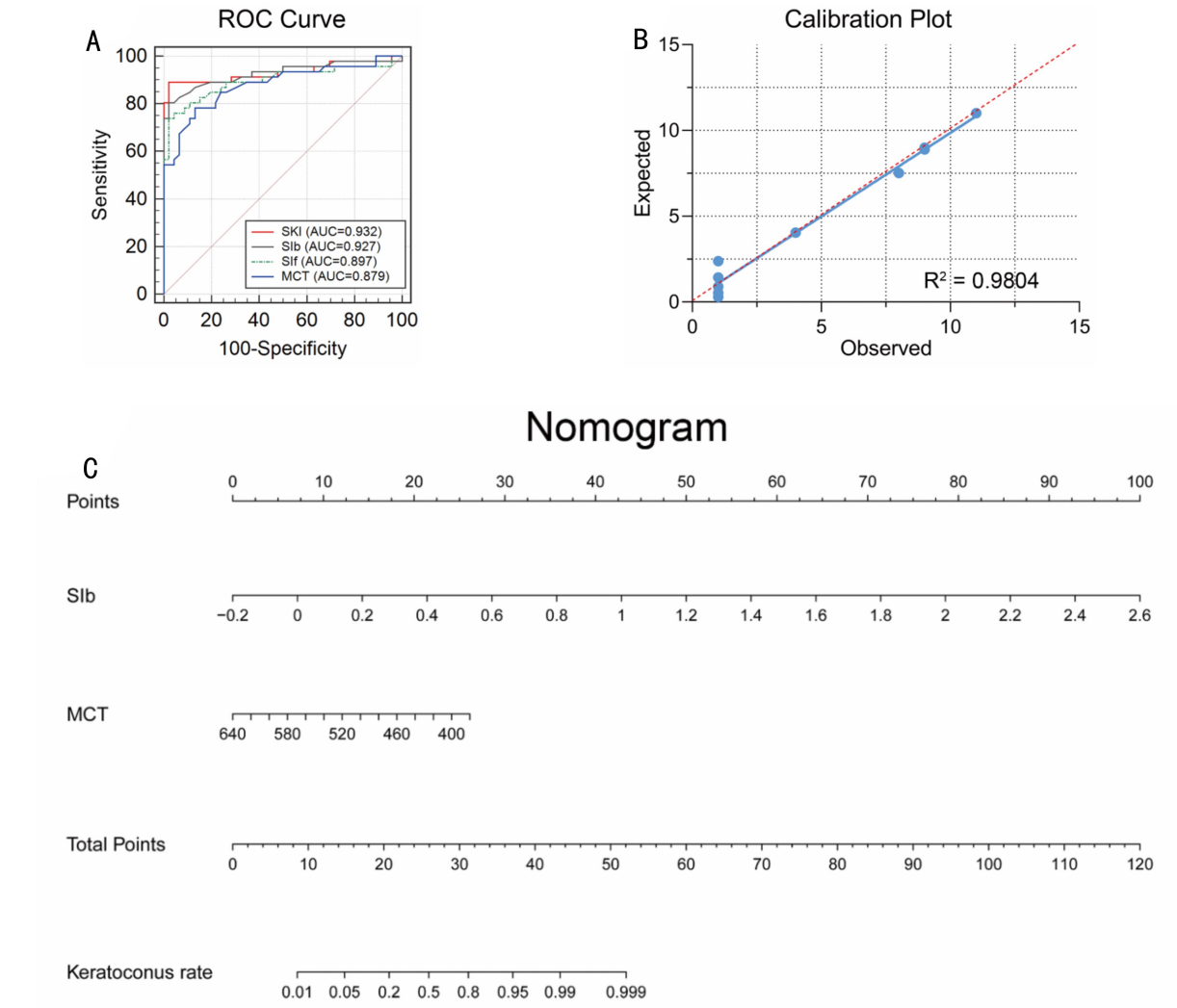

Figure 3 ROC curve, calibration plot and nomogram of the formula in prediction cohort.

red dotted line as the reference line. The curve of the prediction group slightly deviated from the reference line and showed a good calibration of the formula (R^2 = 0.9804) (Figure 3B). A nomogram was constructed based on the two parameters (SIb and MCT) in the formula. When using it, drawing a vertical line from each parameter upward to the points and then recording the corresponding points. The point of each parameter was then summed up to calculate a total score which corresponds to a predicted probability of keratoconus at the bottom of the nomogram (Figure 3C).

ROC curve: Receiver Operating Characteristic curve; SIb: Symmetry index back; SIf: Symmetry index front; MCT: Minimum corneal thickness; LASSO: Least Absolute Shrinkage and Selection Operator; SKI: Sirius Keratoconus Index; AUC: Area under curve.

Overall Comparison between Keratoconus and Normal Groups in the Application Cohort The accuracy of SKI was tested in the application group, which included 23 early KC patients (23 eyes) categorized as suspected KC by Sirius and 23 normal subjects (23 eyes). The demographic and formula - related information of the application group is presented in Table 4. The age (P = 0.834), gender (P = 1.000), average K (P = 0.334) and cylinder (P = 0.886) were comparable between the KC and normal groups. SIb, MCT and SKI showed significant differences between the two groups (P < 0.05). The trends in differences in these parameters were similar in both the prediction and application groups.

ROC Curve and Calibration Analyses in the Application Cohort The ROC curve analysis delineated the sensitivity and specificity of the SIb and MCT in the formula and SKI (Figure 4A). The AUC of SKI (AUC = 0.987) was the highest amongst the parameters in the application group. Additionally, calibration plot was constructed for the application group, using red dotted line as the reference (Figure 4B). The validation of SKI, by Hosmer-Lemeshow test and AUC, suggested a good calibration estimation in 94% of cases in the application group. The accuracy of SKI derived from prediction cohort was examined in the application cohort; the sensitivity was 91% (21/23) and the specificity was 96% (22/23).

The ROC curve analysis delineated the sensitivity and specificity of the 2 parameters (SIb and MCT) in the formula and SKI. SKI (AUC = 0.987) had the highest AUC among these 3 parameters (Figure 4A). Calibration plot was also constructed in application group, with the red dotted line as

Table 4 Comparative demographic and formula-related information in the application cohort

Parameters	Keratoconus group	Normal group	*P*
Number (eyes)	23	23	
Age (years)	26.00 (21.00, 31.00)	25.00 (21.00, 31.00)	0.834
Sex (male: female)	16:7	16:7	1.000
Average K (D)	43.59 (42.15, 44.89)	43.11 (41.88, 43.97)	0.334
Cylinder (D)	-1.25 (-2.27, -0.98)	-1.66 (-2.09, -0.87)	0.886
MCT (μm)	496.00 (471.00, 511.00)	544.00 (515.00, 574.00)	<0.001
SIb (D)	0.43 (0.28, 0.80)	0.04 (-0.04, 0.11)	<0.001
SKI	0.87±0.19	0.17±0.17	<0.001

MCT: Minimum corneal thickness; SIb: Symmetry index back; SKI: Sirius Keratoconus Index.

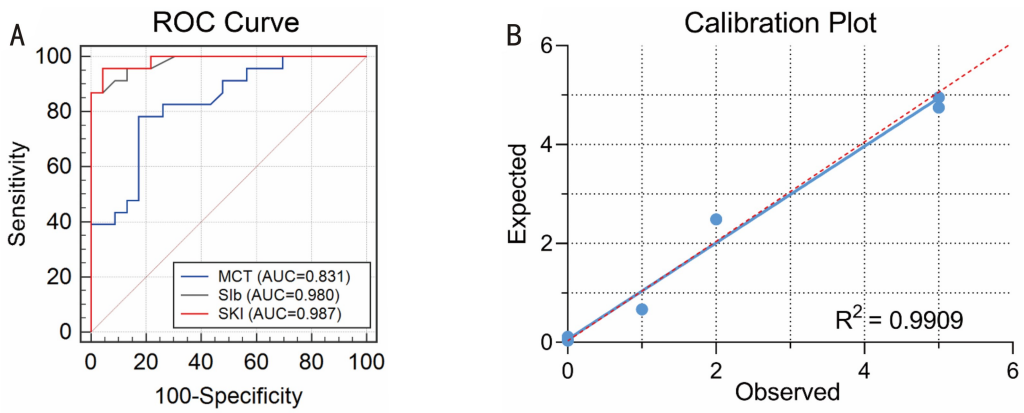

Figure 4 ROC curve and calibration plot of the formula in application cohort.

the reference line. The curve of the application group slightly deviated from the reference line and showed a good calibration of SKI in 94% of cases (R^2=0.9909) (Figure 4B).

ROC curve: Receiver Operating Characteristic curve; SIb: Symmetry index back; MCT: Minimum corneal thickness; SKI: Sirius Keratoconus Index; AUC: Area under curve.

DISCUSSION

Diagnosis of early KC remains a challenge for ophthalmologists especially in patients with suspected KC. Early signs of KC include displacement of the thinnest corneal point from the center, changes in corneal thickness, distribution of epithelial cells, and anterior and posterior corneal astigmatism[16]. Consequently, technologies for detecting these early signs are crucial for early diagnosis of KC. Technologies for characterization, visualization and evaluation of anterior and posterior surfaces of the cornea are vital for early diagnosis of KC. Reflection - based topography and elevation - based systems should be used in combination with high - order aberration measurements to improve the diagnosis of early KC. Ultra-high resolution ultrasound can detect early KC based on the measurements of corneal epithelial and stromal thickness maps[17]. Optical coherence tomography used to measure corneal and epithelial thickness is considered as an advanced technique for early diagnosis of KC[18]. Corneal biomechanics should also be taken into consideration to evaluate the relationship between central corneal thickness and corneal hysteresis[19].

Sirius, a combination of reflection - and elevation - based systems, is a promising technology for early detection of KC[20]. Using maximal depth of focus and with minimal distortion of image, Sirius provides comprehensive information from the anterior corneal surface to the posterior lens surface[9-11,21]. Although Sirius provides several parameters for the evaluation of cornea, early diagnosis of KC still remains a challenge in pre-operative screening in refractive surgery[22]. In the present study, we constructed a prediction formula and evaluated the probability of KC using SKI based on measurements of posterior corneal surface and the thinnest corneal thickness using Sirius.

In previous reports, there is a significant difference in age[23] and gender[24] between KC patients and the healthy subjects; In this study, we addressed these differences by selecting age-and gender-matched normal groups for the corresponding KC groups[25]. There were no significant differences in age and gender between KC and normal group in prediction or application cohort, thus bias due age and gender was prevented. The average K (P=0.334) and cylinder (P=0.886) were also comparable between the two groups in application cohort. This indicated that early KC eyes categorized as suspected KC by Sirius had similar averages of K and cylinder as normal people. Thus, a sensitive index like SKI was needed to differentiate early KC from normal eyes.

In this study, we constructed a Logistic model and nomogram to distinguish the early KC from normal eyes. SIb and MCT were selected as explanatory parameters to predict the early KC eyes. SIb is the difference of average posterior tangential

curvature between two rounded regions centered on the vertical axis in the inferior and superior hemispheres. A positive value indicates steepness in the inferior region, whereas a negative value indicates steepness in the superior region[26]. MCT is the thinnest value of corneal thickness calculated within an 8mm zone. Abnormal posterior corneal surface and alteration in corneal thickness are important for keratoconus diagnosis[6,27]. Previous studies suggest that posterior corneal parameter and minimum corneal thickness are the most distinguishing parameters for early KC and normal eyes and our results were in concordance with these studies[28-29].

The external validation of SKI, with ROC curve (AUC = 0.987) and Hosmer - Lemeshow test (R^2 = 0.9909), suggested a good calibration estimation in 94% of cases in application group. The accuracy of SKI derived from prediction cohort was examined using the external validation cohort with the cut-off of 0.44. The sensitivity was 91% (21/23) and the specificity was 96% (22/23). Shetty *et al*[20] suggest P8 RMS/A as the best parameter of Sirius to detect subclinical keratoconus (AUC=0.730). Heidari *et al*[11] suggest BCVf as the most accurate parameter in Sirius to diagnose subclinical KC (AUC=0.887). Martínez-Abad *et al*[30] suggest ocular residual astigmatism (AUC=0.727) and topography disparity (AUC = 0.756) in Sirius as the promising parameters for diagnosis of subclinical keratoconus. However, our model with SKI based on both MCT and SIb (AUC=0.932 in prediction group and AUC = 0.987 in application group) had greater efficacy and better performance. Additionally, we validated our method in a separate cohort. Arbelaez *et al*[26] constructed a support vector machine (SVM) classifier to analyze curvature, thickness and height data of both the anterior and posterior corneal surfaces and pachymetry in Sirius. The sensitivity and specificity of SVM was 92% and 98%, respectively. These values were similar to those obtained using SKI in the present study (sensitivity and specificity, 91% and 96%, respectively). Additionally, our results were also validated in an external validation cohort.

However, the present study has certain limitations. The sample size was limited as the number of early KC eyes was lesser than KC eyes. The early diagnostic parameters for KC differed significantly in the different devices and thus could not be used interchangeably for the diagnosis of early KC. However, SKI developed is efficient in differentiating early KC from normal eyes and, further studies are needed to validate this formula and the index in multi-center clinical studies.

CONCLUSION

In the present study, we constructed the diagnostic formula and SKI to differentiate early KC eyes from normal eyes in the prediction cohort. ROC curve, calibration plot and nomogram of the formula were systematically analyzed in the prediction cohort. Additionally, external validation of SKI was performed in application cohort. Our findings provide a simple and an effective index for early diagnosis of KC in preoperative screening for refractive surgery.

REFERENCES

1 Ionescu IC, Corbu CG, Tanase C, Ionita G, Nicula C, Coviltir V, Potop V, Constantin M, Codrici E, Mihai S, Popescu ID, *et al*. Overexpression of tear inflammatory cytokines as additional finding in keratoconus patients and their first degree family members. *Mediators Inflamm* 2018;2018:4285268

2 Karamichos D. Keratoconus: challenges and emerging trends. *J Mol Genet Med* 2018;12(3):367

3 Mas Tur V, MacGregor C, Jayaswal R, O'Brart D, Maycock N. A review of keratoconus: Diagnosis, pathophysiology, and genetics. *Surv Ophthalmol* 2017;62(6):770-783

4 Fernández Pérez J, Valero Marcos A, Martínez Peña FJ. Early diagnosis of keratoconus: what difference is it making? *Br J Ophthalmol* 2014;98(11):1465-1466

5 Kojima T, Nishida T, Nakamura T, Tamaoki A, Hasegawa A, Takagi Y, Sato H, Ichikawa K. Keratoconus screening using values derived from auto-keratometer measurements: a multicenter study. *Am J Ophthalmol* 2020;215:127-134

6 Randleman JB, Dupps WJ Jr, Santhiago MR, Rabinowitz YS, Koch DD, Stulting RD, Klyce SD. Screening for keratoconus and related ectatic corneal disorders. *Cornea* 2015;34(8):e20-e22

7 Reddy JC, Rapuano CJ, Cater JR, Suri K, Nagra PK, Hammersmith KM. Comparative evaluation of dual Scheimpflug imaging parameters in keratoconus, early keratoconus, and normal eyes. *J Cataract Refract Surg* 2014;40(4):582-592

8 Velázquez JS, Cavas F, Piñero DP, Cañavate FJF, Alio del Barrio J, Alio JL. Morphogeometric analysis for characterization of keratoconus considering the spatial localization and projection of apex and minimum corneal thickness point. *J Adv Res* 2020;24:261-271

9 Montalbán R, Alio JL, Javaloy J, Piñero DP. Comparative analysis of the relationship between anterior and posterior corneal shape analyzed by Scheimpflug photography in normal and keratoconus eyes. *Graefes Arch Clin Exp Ophthalmol* 2013;251(6):1547-1555

10 Prakash G, Suhail M, Srivastava D. Predictive analysis between topographic, pachymetric and wavefront parameters in keratoconus, suspects and normal eyes: creating unified equations to evaluate keratoconus. *Curr Eye Res* 2016;41(3):334-342

11 Heidari Z, Mohammadpour M, Hashemi H, Jafarzadehpur E, Moghaddasi A, Yaseri M, Fotouhi A. Early diagnosis of subclinical keratoconus by wavefront parameters using Scheimpflug, Placido and Hartmann-Shack based devices. *Int Ophthalmol* 2020; 40(7): 1659-1671

12 Xie Y, Zhao LQ, Yang XN, Wu XH, Yang YH, Huang XM, Liu F, Xu JP, Lin LM, Lin HQ, Feng QT, *et al*. Screening candidates for refractive surgery with corneal tomographic-based deep learning. *JAMA Ophthalmol* 2020;138(5):519-526

13 Vasquez MM, Hu CC, Roe DJ, Chen Z, Halonen M, Guerra S. Least absolute shrinkage and selection operator type methods for the identification of serum biomarkers of overweight and obesity: simulation and application. *BMC Med Res Methodol* 2016;16:154

14 Xu WH, Xu Y, Tian X, Anwaier A, Liu WR, Wang J, Zhu WK, Cao DL, Wang HK, Shi GH, Qu YY, *et al*. Large-scale transcriptome profiles reveal robust 20-signatures metabolic prediction models and novel role of G6PC in clear cell renal cell carcinoma. *J Cell Mol Med* 2020;24(16):9012-9027

15 Hou JY, Wang YG, Ma SJ, Yang BY, Li QP. Identification of a prognostic 5-Gene expression signature for gastric cancer. *J Cancer Res Clin Oncol* 2017;143(4):619-629

16 Awad Eman A., Abou Samra Waleed A., Torky Magda A., El-Kannishy Amr M. Objective and subjective diagnostic parameters in the fellow eye of unilateral keratoconus. *BMC Ophthalmol*, 2017;17(1):186

17 Reinstein Dan Z., Archer Timothy J., Urs Raksha., Gobbe Marine., RoyChoudhury Arindam., Silverman Ronald H. Detection of Keratoconus in Clinically and Algorithmically Topographically Normal Fellow Eyes Using Epithelial Thickness Analysis. *J Refract Surg*, 2015; 31(11):736-744

18 Yip H, Chan E. Optical coherence tomography imaging in keratoconus. *Clin Exp Optom* 2019;102(3):218-223

19 Catalún-López S, Cadarso-Suárez L, López-Ratón M, Cadarso-Suárez C. Corneal biomechanics in unilateral keratoconus and fellow eyes with a scheimpflug-basedtonometer. *Optom Vis Sci* 2018; 95(7): 608-615

20 Shetty R, Rao H, Khamar P, Sainani K, Vunnava K, Jayadev C, Kaweri L. Keratoconus screening indices and their diagnostic ability to distinguish normal from ectatic corneas. *Am J Ophthalmol* 2017; 181: 140-148

21 Finis D, Ralla B, Karbe M, Borrelli M, Schrader S, Geerling G. Comparison of two differentscheimpflug devices in the detection of keratoconus, regular astigmatism, and healthy corneas. *J Ophthalmol* 2015;2015:315281

22 Imbornoni LM, McGhee CNJ, Belin MW. Evolution of keratoconus: from diagnosis to therapeutics. *Klin Monbl Augenheilkd* 2018;235(6): 680-688

23 Kocamış Si, Çakmak HB, Çağıl N, Toklu Y. Investigation of the efficacy of the cone location and magnitude index in the diagnosis of keratoconus. *Semin Ophthalmol* 2016;31(3):203-209

24 Sidky MK, Hassanein DH, Eissa SA, Salah YM, Lotfy NM. Prevalence of subclinical keratoconus among pediatric Egyptian population with astigmatism. *Clin Ophthalmol* 2020;14:905-913

25 Woodward MA, Blachley TS, Stein JD. The association between sociodemographic factors, common systemic diseases, and keratoconus: an analysis of a nationwide heath care claims database. *Ophthalmology* 2016;123(3):457-465.e2

26 Arbelaez MC, Versaci F, Vestri G, Barboni P, Savini G. Use of a support vector machine for keratoconus and subclinical keratoconus detection by topographic and tomographic data. *Ophthalmology* 2012;119(11):2231-2238

27 Altinkurt E, Avci O, Muftuoglu O, Ugurlu A, Cebeci Z, Ozbilen KT. Logistic regression model usingscheimpflug-placido cornea topographer parameters to diagnose keratoconus. *J Ophthalmol* 2021;2021:5528927

28 Safarzadeh M, Nasiri N. Anterior segment characteristics in normal and keratoconus eyes evaluated with a combined Scheimpflug/Placido corneal imaging device. *J Curr Ophthalmol* 2016;28(3):106-111

29 Belin MW, Jang HS, Borgstrom M. Keratoconus: diagnosis and staging. *Cornea* 2022;41(1):1-11

30 Martínez-Abad A, Piñero DP, Ruiz-Fortes P, Artola A. Evaluation of the diagnostic ability of vector parameters characterizing the corneal astigmatism and regularity in clinical and subclinical keratoconus. *Contact Lens Anterior Eye* 2017;40:88-96